ACS central science

Research Article

http://pubs.acs.org/journal/acscii

Molecular Motor Dnm1 Synergistically Induces Membrane Curvature To Facilitate Mitochondrial Fission

Michelle W. Lee,[†] Ernest Y. Lee,[†] Ghee Hwee Lai,[†,‡] Nolan W. Kennedy,[§] Ammon E. Posey,[∥] Wujing Xian,[†] Andrew L. Ferguson,[⊥,#] R. Blake Hill,[*,§] and Gerard C. L. Wong[*,†,¶,⊗]

[†]Department of Bioengineering, [¶]Department of Chemistry & Biochemistry, and [⊗]California NanoSystems Institute, University of California, Los Angeles, Los Angeles, California 90095, United States

[⊥]Department of Materials Science and Engineering and [#]Department of Chemical and Biomolecular Engineering, University of Illinois at Urbana−Champaign, Urbana, Illinois 61801, United States

[§]Department of Biochemistry, Medical College of Wisconsin, Milwaukee, Wisconsin 53226, United States

[∥]Department of Biomedical Engineering, Washington University in St. Louis, St. Louis, Missouri 63130, United States

Supporting Information

ABSTRACT: Dnm1 and Fis1 are prototypical proteins that regulate yeast mitochondrial morphology by controlling fission, the dysregulation of which can result in developmental disorders and neurodegenerative diseases in humans. Loss of Dnm1 blocks the formation of fission complexes and leads to elongated mitochondria in the form of interconnected networks, while overproduction of Dnm1 results in excessive mitochondrial fragmentation. In the current model, Dnm1 is essentially a GTP hydrolysis-driven molecular motor that self-assembles into ring-like oligomeric structures that encircle and pinch the outer mitochondrial membrane at sites of fission. In this work, we use machine learning and synchrotron small-angle X-ray scattering (SAXS) to investigate whether the motor Dnm1 can synergistically facilitate mitochondrial fission by membrane remodeling. A support vector machine (SVM)-based classifier trained to detect sequences with membrane-restructuring activity identifies a helical Dnm1 domain capable of generating negative Gaussian curvature (NGC), the type of saddle-shaped local surface curvature found on scission necks during fission events. Furthermore, this domain is highly conserved in Dnm1 homologues with fission activity. Synchrotron SAXS measurements reveal that Dnm1 restructures membranes into phases rich in NGC, and is capable of inducing a fission neck with a diameter of 12.6 nm. Through *in silico* mutational analysis, we find that the helical Dnm1 domain is locally optimized for membrane curvature generation, and phylogenetic analysis suggests that dynamin superfamily proteins that are close relatives of human dynamin Dyn1 have evolved the capacity to restructure membranes via the induction of curvature mitochondrial fission. In addition, we observe that Fis1, an adaptor protein, is able to inhibit the pro-fission membrane activity of Dnm1, which points to the antagonistic roles of the two proteins in the regulation of mitochondrial fission.

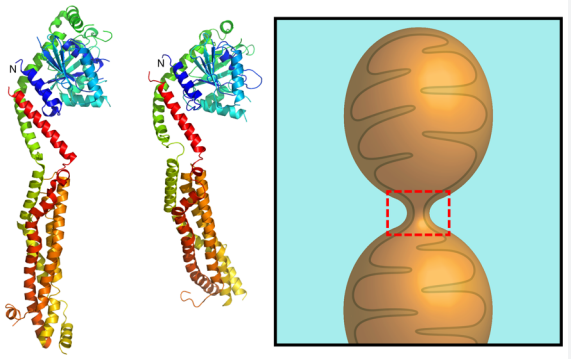

The morphology and distribution of mitochondria, which vary among different cell types[1] and respond to different cellular conditions,[2−5] are crucial for maintaining normal cell function.[6] Mitochondrial morphology and intracellular distribution are primarily governed by a balance between the antagonistic processes of fusion and fission.[7−9] Excessive fusion results in elongated mitochondria that form highly interconnected net-like structures, whereas uninhibited fission leads to mitochondrial fragmentation.[7,10−12] Recent studies have associated perturbations in these dynamic processes with developmental defects and neurodegenerative diseases.[12−14] Proteins that regulate and maintain mitochondrial morphology, therefore, play important roles in health and disease.

The machinery involved in mitochondrial fission was first identified in yeast to include Dnm1 and Fis1,[6,9,11,15] with Drp1 and hFis1 as their respective conserved human homologues.[10,16−19] A highly conserved cytosolic dynamin-related GTPase, Dnm1 (∼85 kDa) in yeast *Saccharomyces cerevisiae* and Drp1 (∼82 kDa) in mammals, is the major essential protein involved in eukaryotic mitochondrial fission.[9] Loss of Dnm1/Drp1 blocks the formation of fission complexes[15,20] and results in the formation of net-like structures.[6,8,9] Likewise, mutations in Dnm1 homologues were also shown to block fission,[17,21] while overproduction of Dnm1 leads to increased mitochondrial fragmentation.[22] Dnm1/Drp1 is characterized by an N-terminal GTPase, a middle domain, and a C-terminal GTPase effector domain involved in self-assembly.[7,23] In the

Received: July 27, 2017
Published: November 8, 2017

DOI: 10.1021/acscentsci.7b00338
ACS Cent. Sci. 2017, 3, 1156−1167

current model, Dnm1/Drp1 is essentially a molecular motor recruited from the cytosol and self-assembles into spiral-like or ring-like oligomeric structures that encircle the outer mitochondrial membrane at sites of fission. GTP hydrolysis leads to Dnm1/Drp1 conformational changes that constrict the membranes to drive membrane scission.[24−28]

The process of budding and scission, however, requires the generation of significant local negative Gaussian curvature (NGC) in membranes.[29] NGC is the saddle-shaped membrane surface curvature found in the pinched regions of mitochondria undergoing fission. Interestingly, recent work has indicated that specific membrane lipids can facilitate mitochondrial fission,[29−33] and that lipids can play a role in binding, recruiting, and activating proteins that mediate fission, including Drp1.[29,34−36] For example, a cryo-EM study has shown that the active helical conformation of Drp1 is stabilized through direct interactions with cardiolipin.[37] Furthermore, studies have shown that induced membrane curvature via protein crowding can also facilitate membrane fission.[38−40] In this work, we use machine learning and synchrotron small-angle X-ray scattering (SAXS) to investigate whether Dnm1−lipid interactions can play a role in facilitating mitochondrial membrane remodeling and fission. To assess whether Dnm1 contains subdomains that can potentially induce membrane curvature necessary for scission, we screen the protein using a recently developed machine-learning-based classifier[41] that predicts whether a given α-helical peptide sequence can generate NGC. (The machine learning was performed on α-helical sequences.) Using this classifier, we find a high-scoring N-terminal α-helical domain (LEDLIPTVNKLQDVMYD) in the protein sequence of Dnm1, which suggests that this domain may be able to remodel membranes by generating NGC. Interestingly, this sequence is conserved in Dnm1 homologues with fission activity. To test experimentally whether Dnm1 has the capacity to facilitate fission by restructuring membranes in a manner synergistic with its molecular-motor-based mitochondrial "pinching" activity, SAXS is used to investigate the full spectrum of Dnm1-induced membrane deformations in vesicles with mitochondrial-like lipid compositions. SAXS results show that Dnm1 indeed restructures membranes into phases rich in NGC, in agreement with the machine-learning results. The capacity to induce NGC suggests that Dnm1 function is more complex than just simply mechanochemical constriction activity mediated by its oligomerization. In fact, the membrane deformations generated by Dnm1 promote fission by rendering membranes more amenable to the restructuring necessary for scission. We find that the observed degree of induced NGC is consistent with a fission neck having a diameter of 12.6 nm. An *in silico* mutational analysis of the N-terminal helix of Dnm1 suggests that it is locally optimized for the induction of membrane curvature. In addition, phylogenetic analysis of dynamin superfamily members reveals that proteins close in mutational distance to human dynamin Dyn1 have evolved the ability to remodel membranes through curvature generation. These results suggest that Dnm1-induced membrane curvature and mechanochemical forces function cooperatively to efficiently catalyze mitochondrial fission, supporting the notion that the fission reaction depends on a combination of both protein and membrane mechanics. Remarkably, we find that the adaptor protein Fis1 inhibits the pro-fission membrane activity of Dnm1 by quantitatively suppressing Dnm1-induced NGC. Based on these antagonistic qualities of Dnm1 and Fis1, we suggest the possibility that the two proteins work in concert to modulate mitochondrial fission.

RESULTS AND DISCUSSION

Machine Learning Predicts Dnm1 To Contain Membrane-Destabilizing Sequences. NGC can be described as saddle-splay curvature due to its shape: the surface curves upward in one direction and downward in the orthogonal direction. This specific type of curvature is topologically required for membrane-destabilizing processes, such as budding and pore formation. Moreover, it is the type of local surface curvature found on scission necks during fission events.[42−44] (The pinched fission neck is a classic example of NGC.) A large body of work has identified short peptides that can sense[45] or induce membrane curvature and remodeling.[45−49] Membrane active subsequences derived from viral fusion and fission proteins have been shown to disrupt and bend lipid bilayers.[46,50,51] In fact, for peptides that function through membrane destabilization, a strong correlation has been found between their ability to generate NGC and their activity.[42] For example, NGC generation has been experimentally observed using SAXS for antimicrobial peptides (AMPs),[42,52−56] cell-penetrating peptides (CPPs),[43,57−59] and viral fusion and fission proteins.[60,61] These findings collectively suggest that generation of NGC is important in membrane-destabilizing processes.

To assess whether Dnm1 contains subdomains that may induce membrane curvature important for fission, we employed a recently developed machine-learning classifier trained to predict the likelihood of membrane-restructuring activity for a given α-helical peptide sequence.[41] This classifier, which was originally trained with AMP sequences, has been shown to be a good detector of NGC-generating α-helical domains in diverse families of proteins, including membrane-active segments of viral fusion proteins and endocytosis/exocytosis proteins. More notably, its effectiveness in detecting membrane-destabilizing activity in peptide sequences allows for the recognition of previously undetected membrane activity in existing proteins or peptides, such as the neuropeptide hormones.[41]

The classifier is based on a linear support vector machine (SVM) that takes as input $n = 12$ physicochemical descriptors generated from the peptide sequence and outputs a score σ specifying the distance of the peptide from an $(n - 1) = 11$ dimensional hyperplane trained to optimally separate 243 known α-helical curvature-generating peptides from 243 decoy peptides. A large, positive σ score correlates with increased ability to induce NGC in membranes, whereas a negative σ score indicates a lack of membrane-disruptive activity. This score can be converted through a monotonic function into a probability $0 < P(+1) < 1$ that the peptide induces membrane curvature. Large, positive values of σ ($P(+1) > 0.95$) indicate a high likelihood of membrane activity (ability to generate NGC), and negative values of σ ($P(+1) < 0.50$) indicate a low probability of membrane activity. Testing of the classifier on a blind balanced test set of 86 peptides demonstrated 91.9% prediction accuracy, 93.0% specificity, and 90.7% sensitivity. Experimental validation of computational predictions was carried out using SAXS. A subset of α-helical test peptides were incubated with model membranes, and induced NGC was measured. A strong correlation between the ability to generate NGC in membranes and the distance-to-hyperplane SVM metric σ was observed. Classification of a single peptide requires ∼0.1 s of CPU time permitting high-throughput computational screening for membrane-active peptide discov-

DOI: 10.1021/acscentsci.7b00338
ACS Cent. Sci. 2017, 3, 1156−1167

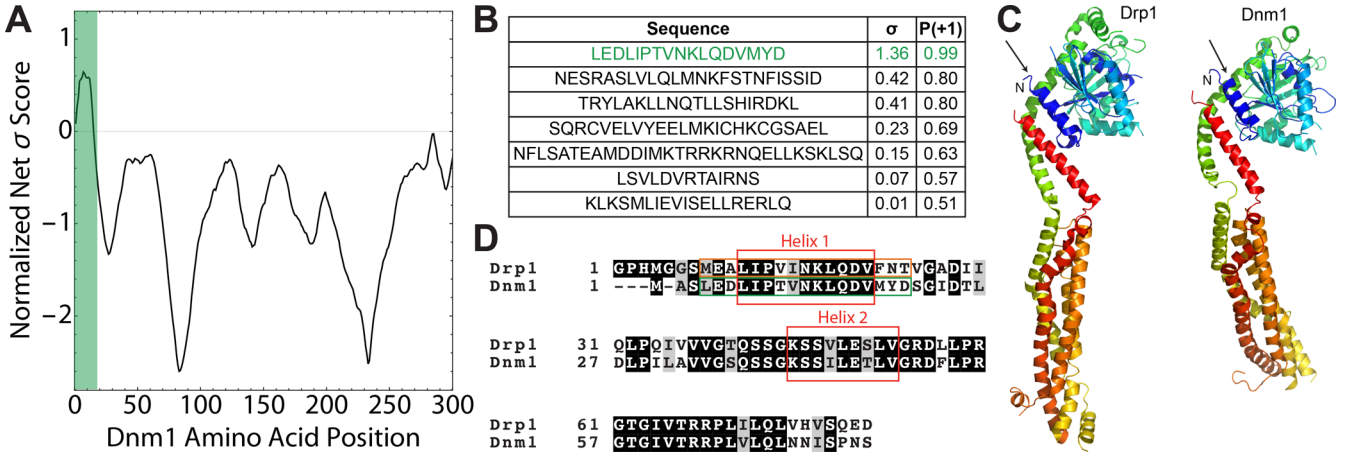

Figure 1. Machine-learning screen of Dnm1 yields a putative membrane-destabilizing sequence in the conserved N-terminal domain. (A) Normalized σ scores of a moving-window scan of Dnm1 for membrane activity as a function of amino acid position. Scores are shown for the first 300 amino acids of Dnm1. The green bar highlights the location of the top-scoring helical subsequence of Dnm1. (B) Table showing the top-scoring helical subsequences from Dnm1 with $\sigma > 0$ and their corresponding σ and $P(+1)$ assignments from the machine-learning classifier. The top hit LEDLIPTVNKLQDVMYD corresponds to a segment of Dnm1 that contains the first N-terminal helix (highlighted in panel A). This sequence has a $P(+1)$ score >95%, which indicates a high likelihood of NGC generation and membrane restructuring ability. (C) 3D homology structure model of yeast Dnm1 (UniProtKB: P54861) (right) based on the known crystal structure of human Drp1 (PDB: 4BEJ) (left). The first N-terminal helices in both protein sequences are depicted in blue and indicated by the arrows. (D) Sequence alignment of the N-terminal regions of Drp1 and Dnm1 shows significant sequence homology and conservation. The first two conserved N-terminal helices in both sequences are boxed in red. The sequence boxed in green (LEDLIPTVNKLQDVMYD) corresponds to the top hit from the machine-learning screen for membrane-destabilizing segments of Dnm1, while the corresponding aligned sequence from Drp1 is boxed in orange (MEALIPVINKLQDVFNT).

ery and design. Full details of data set curation, physicochemical descriptor selection, and model training and validation is provided in refs 41 and 62.

We use the classifier to evaluate whether Dnm1 contains amino acid sequences that might remodel membranes through membrane curvature induction. To locate potential curvature-generating domains in Dnm1 (UniProtKB: P54861), we enumerated all possible 10−25 amino acid subsequences of the entire protein sequence and performed a moving window scan with the membrane activity prediction tool. To visualize the membrane activity landscape along the length of Dnm1, a normalized net σ score was calculated by aligning all windowed sequences and averaging over σ values (Figure 1A). Maxima at positive σ values in this landscape correspond to subsequences that have high likelihood of membrane activity. In conjunction with this scan, we predicted the secondary structure of Dnm1 using two methods: the DSSP secondary structure prediction algorithm[63] and sequence alignment with the known crystal structure of human homologue Drp1 (PDB: 4BEJ).[64] Surprisingly, when we compared the results of the moving window scan with the secondary structure prediction (Figure S1), we found a membrane-destabilizing α-helical sequence (LEDLIPTVNKLQDVMYD, σ = 1.36, $P(+1)$ = 0.99) with an exceedingly high score (Figure 1B). This sequence lies in a highly conserved N-terminal region shared with Dnm1 homologues that also have membrane activity (Figure 1C,D; Figure S5). Likewise, the corresponding aligned sequence for Drp1 was also predicted to be membrane-destabilizing (MEALIPVINKLQDVFNT, σ = 1.51, $P(+1)$ = 0.99). In addition to this sequence, the algorithm predicted six other helices of Dnm1 to potentially possess membrane activity, but with lower confidence ($P(+1) < 0.95$). These machine-learning results predict that Dnm1 contains multiple α-helical sequences with potential membrane-destabilizing activity, including one particularly high scoring domain (Figure 1B). These findings from machine learning suggest the testable hypothesis that, in addition to promoting mitochondrial fission through mechanochemical constriction activity, the GTPase-driven molecular motor Dnm1 may have the capacity to enhance mitochondrial fission through induced NGC membrane deformations.

Dnm1 Remodels Membranes and Induces Negative Gaussian Curvature To Promote Mitochondrial Membrane Fission. To test the predictions from the machine-learning classifier, we assessed the ability of Dnm1 to generate membrane-destabilizing curvature. Using high-resolution synchrotron SAXS, we quantitatively characterized Dnm1-induced membrane deformations in model mitochondrial membranes. Small unilamellar vesicles (SUVs) were prepared from ternary phospholipid mixtures of phosphatidylethanolamine (PE), phosphatidylcholine (PC), and cardiolipin (CL) at molar ratios of 75/15/10 and 75/5/20 to mimic the lipid compositions of mitochondrial membranes.[30,35,65−67] Dnm1 was incubated with SUVs at a protein-to-lipid (P/L) molar ratio of 1/1000, and the resulting membrane structures were characterized using SAXS. The Dnm1 concentrations used were comparable to those used in a large number of prior Dnm1−lipid interaction studies (0.2−10 μM).[25,27,31,64,68−70]

We found that Dnm1 restructured the lipid vesicles into phases rich in NGC, while the control samples of SUVs only showed a broad characteristic feature consistent with the form factor of unilamellar vesicles (Figure S2). For the model membrane 75/15/10 PE/PC/CL, we observed a coexistence of two phases: (1) one set of correlation peaks with Q-ratios $\sqrt{1}:\sqrt{3}:\sqrt{4}:\sqrt{7}:\sqrt{9}$, consistent with an inverted hexagonal (H_{II}) phase with a lattice parameter of 7.88 nm; (2) a second set of peaks with Q-ratios $\sqrt{2}:\sqrt{3}:\sqrt{4}:\sqrt{6}:\sqrt{8}:\sqrt{9}:\sqrt{10}$, which indexed to a *Pn*3*m* "double-diamond" cubic (Q_{II}) phase with a lattice parameter of 34.16 nm (Figure 2). Similarly, the model membrane 75/5/20 PE/PC/CL exhibited H_{II} and *Pn*3*m* Q_{II} phases with lattice parameters of 7.70 and 16.15 nm, respectively. However, for this membrane composition, an additional third set of peaks was identified,

DOI: 10.1021/acscentsci.7b00338
ACS Cent. Sci. 2017, 3, 1156−1167

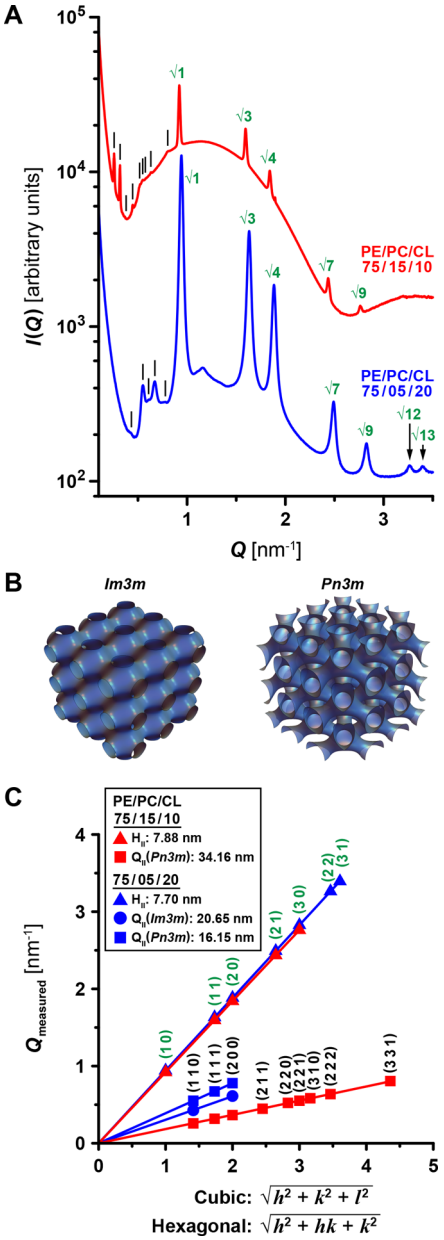

Figure 2. Dnm1 generates NGC necessary for mitochondrial membrane fission. (A) SAXS spectra from 75/15/10 and 75/5/20 PE/PC/CL model mitochondrial membranes incubated with Dnm1 at $P/L = 1/1000$. Correlation peaks corresponding to assigned reflections are indicated for hexagonal (green) and cubic (black lines) phases. (B) 3D reconstructions depicting *Im3m* (left) and *Pn3m* (right) cubic phases, which have continuous surfaces with NGC at every point. (C) Indexing of Dnm1-induced H_{II}, and *Pn3m* and *Im3m* Q_{II} phases for 75/15/10 (red) and 75/5/20 (blue) PE/PC/CL membranes. Plots of the measured Q positions, $Q_{measured}$, versus the assigned reflections in terms of Miller indices, $\sqrt{h^2 + hk + k^2}$ for hexagonal and $\sqrt{h^2 + k^2 + l^2}$ for cubic phases. The lattice parameters were calculated from the slopes of the linear regressions through the points and are provided in the legend.

which indexed to an *Im3m* "plumber's nightmare" Q_{II} phase with a lattice parameter of 20.65 nm. These coexisting *Pn3m* and *Im3m* Q_{II} phases for this membrane had lattice parameters with a ratio close to the Bonnet ratio of 1.279,[71] indicating that they are near equilibrium with the quantitative amount of membrane curvature balanced between the two cubic phases. Additional measurements on phosphatidylserine (PS)-containing SUVs incubated with Dnm1 having a maltose-binding protein (MBP) tag also showed the induction of H_{II} and *Im3m* Q_{II} phases, indicating that the NGC-generating activity is robust, consistent with earlier findings that MBP, or other N-terminal fusion tags like GFP, do not interfere with Dnm1 activity[68,72,73] (Figure S3). A bicontinuous cubic phase, such as *Pn3m* and *Im3m*, consists of two nonintersecting aqueous regions that are separated by a lipid bilayer. The center of this bilayer traces out a periodic minimal surface that has NGC at every point. From our SAXS measurements, we found that Dnm1 promotes saddle-shaped membrane deformations to stabilize bulk cubic phases in model membranes with lipid compositions that closely resemble those of mitochondrial membranes, but not others (data not shown). These observations of a strong Dnm1-induced propensity to restructure a lamellar bilayer into an NGC-rich cubic phase mirror the required membrane-remodeling events involved in mitochondrial fission. More specifically, NGC promotes membrane deformations that enable the adoption of the unique structures and morphologies that characterize mitochondrial fission. For instance, NGC manifests at the constriction necks of mitochondrial membranes that are formed during the fission process. Remarkably, this intrinsic membrane activity occurs in the absence of GTP binding or hydrolysis, and indicates that Dnm1 may help mediate membrane fission through the induction of NGC in a manner similar to that previously shown by viral scission proteins.[59]

One question to ask is whether the amount of NGC induced by Dnm1 is quantitatively close to the amount found in mitochondrial fission events. We compare the quantitative amount of NGC generated by Dnm1 per unit area with the amount of NGC in a constricted fission membrane neck approximated by a catenoid surface[61,74] (red-dashed box, Figure 3A,B). The average amount of Gaussian curvature, K, in a cubic phase can be calculated using the equation $\langle K \rangle = (2\pi\chi)/(A_0 a^2)$, where a is the lattice parameter. The Euler characteristic, χ, and surface area per unit cell, A_0, are constants specific to each cubic phase. For *Pn3m*, $\chi = -2$ and $A_0 = 1.919$, and for *Im3m*, $\chi = -4$ and $A_0 = 2.345$.[71] For the 75/5/20 PE/PC/CL model membrane, Dnm1 generated *Pn3m* and *Im3m* Q_{II} phases with lattice parameters of 16.15 and 20.65 nm, respectively, which both amount to $\langle K \rangle = -2.5 \times 10^{-2}$ nm^{-2}. The shape of a constricted scission neck is modeled using a catenoid surface (Figure 3B), which is a minimal surface that has Gaussian curvature $K(z) = -\text{sech}^4(z/r)/r^2$, where the r is the radius of the circular cross section along the neck axis, z. We find that a value of $K = -2.5 \times 10^{-2}$ nm^{-2} equates to a constricted membrane neck that has a radius of 6.3 nm at its narrowest point, $z = 0$ (denoted by *, Figure 3B,C). These results show that the Dnm1-induced NGC corresponds to a fission neck of approximately 12.6 nm diameter in the absence of nucleotide. This value is considerably smaller than the neck diameter typically observed using electron microscopy and super-resolution microscopy for Dnm1/Drp1 interacting with model membranes with simplified compositions.[75,76] In fact, neither protein has successfully demonstrated scission of lipid tubes *in vitro*.[24,27,77−79] Although GTP binding is known to further constrict the membrane tubule,[70] this constriction appears insufficient to cause membrane scission. Recent findings demonstrate that dynamin-2 is necessary for the final stages of membrane scission of human mitochondria.[79] Thus, our observation of high membrane curvatures and small fission

DOI: 10.1021/acscentsci.7b00338
ACS Cent. Sci. 2017, 3, 1156−1167

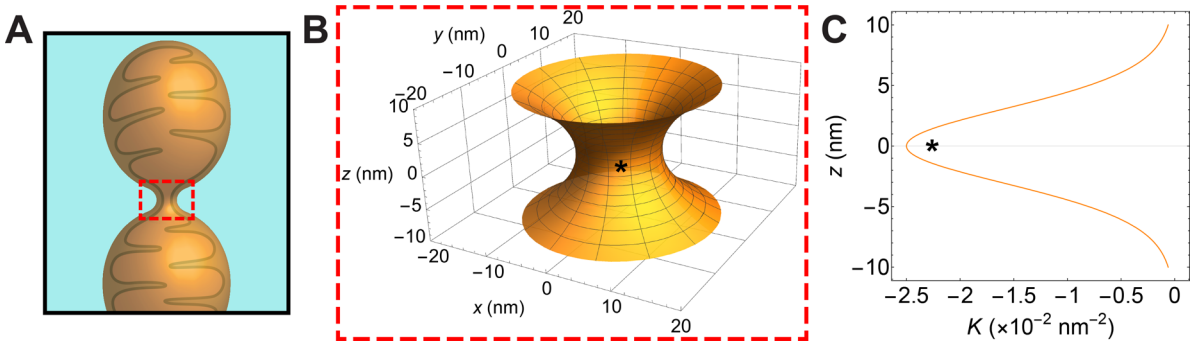

Figure 3. Dnm1-mediated NGC corresponds to a fission neck with a diameter of 12.6 nm. (A) A scission neck (red-dashed box) is formed during the mitochondrial fission process. This structure can be modeled as a catenoid surface, which allows us to estimate the neck size that can be produced by a given quantitative amount of NGC. (B) Schematic of a catenoid surface approximating a mitochondrial fission neck (an enlarged view of the red-boxed region in panel A) with a diameter of 12.6 nm at the narrowest cross section, which occurs at $z = 0$ (indicated by *), where z describes the distance along the catenoid axis (i.e., the length of the neck). (C) A plot of the calculated Gaussian curvature (K) along the surface of the model catenoid as a function of z-distance (nm). Since the catenoid is rotationally symmetric about the z-axis, this describes K everywhere along the surface. Far from the scission neck (e.g., $z = \pm 10$ nm), the Gaussian curvature is near zero. As z approaches the narrowest cross section along the catenoid surface, NGC increases drastically and reaches a maximum value at $z = 0$ (denoted by * in panel B). Maximal NGC (*) corresponds to a value of $K = -2.5 \times 10^{-2}$ nm^{-2}, which is the quantitative amount of NGC observed in the bicontinuous cubic phases generated by Dnm1 in 75/5/20 PE/PC/CL membranes (Figure 2).

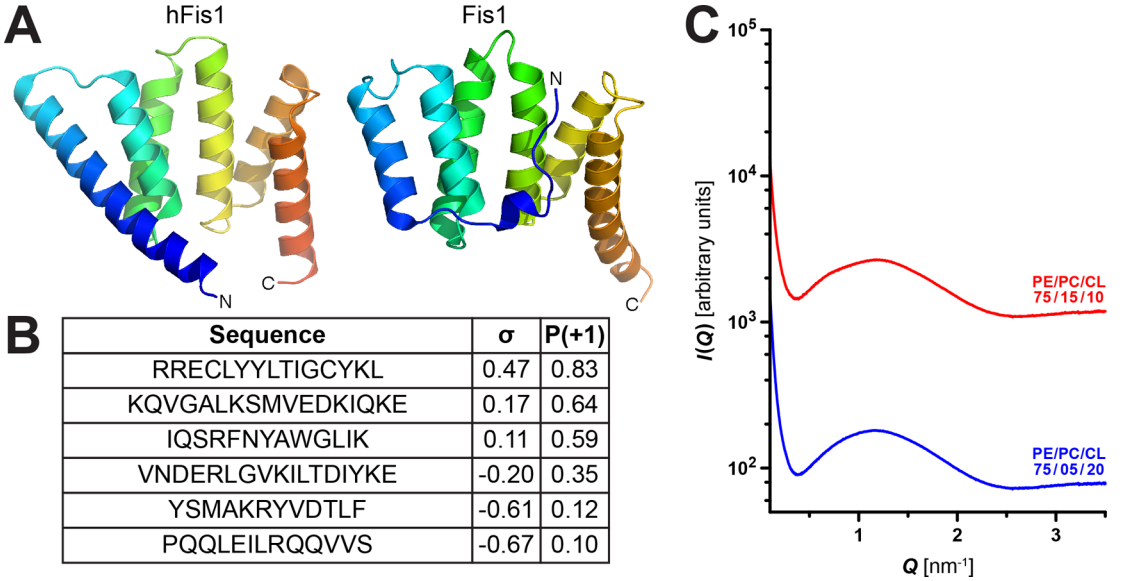

Sequence	σ	P(+1)
RRECLYYLTIGCYKL	0.47	0.83
KQVGALKSMVEDKIQKE	0.17	0.64
IQSRFNYAWGLIK	0.11	0.59
VNDERLGVKILTDIYKE	-0.20	0.35
YSMAKRYVDTLF	-0.61	0.12
PQQLEILRQQVVS	-0.67	0.10

Figure 4. Helix-rich Fis1 is not predicted to destabilize membranes and does not restructure model mitochondrial membranes. (A) 3D structures of yeast Fis1[86] (PDB: 3O48) (right) and human hFis1[100] (PDB: 1NZN) (left) show strongly conserved helical content. Both proteins contain a six-helix array. (B) The six helical subsequences of Fis1 were screened for membrane activity using the machine-learning classifier. A table of the Fis1 helical subsequences with their corresponding outputs σ and $P(+1)$ from the machine-learning screen is reported. Predictions suggest that helical subsequences of Fis1 have a low probability ($P(+1) < 0.95$) of membrane-destabilizing activity and are unlikely to generate NGC. (C) Fis1 at $P/L = 1/500$ showed minimal membrane activity and did not significantly restructure either 75/15/10 or 75/5/20 PE/PC/CL membranes (no generation of NGC). Their SAXS profiles closely resembled those of control samples containing only lipid vesicles (Figure S2).

necks via Dnm1-induced membrane remodeling synergistic to motor-driven membrane constriction is highly suggestive of a composite, mutually-amplifying fission mechanism, and that membranes with a significant portion of negative spontaneous curvature lipids, such as mitochondrial membranes, can be remodeled by Dnm1 into narrower fission necks via NGC generation.

Coupled with evidence implicating key roles for specific membrane lipids in mitochondrial fission, such as the interactions between CL and Drp1 in forming CL-enriched membrane regions[29,35,70,80,81] that may facilitate membrane remodeling[29] and activation of Drp1 GTPase activity,[30,37] the results described here further demonstrate the crucial function of membrane dynamics in the fission process. These findings using synchrotron SAXS, which are in agreement with the machine-learning classifier predictions for the existence of a membrane-active domain that is conserved between Dnm1 and its homologue Drp1, point to the ability of Dnm1 to catalyze mitochondrial fission via its GTPase hydrolysis-driven mitochondrial pinching activity in conjunction with synergistic membrane-remodeling activity.

The results presented here make contact with a key aspect of mitochondrial fission related to Fis1, a protein localized to the outer mitochondrial membrane. Previous studies have suggested that yeast Fis1 recruits Dnm1 from the cytosol to the mitochondrial membrane.[6,73,82] However, other studies

DOI: 10.1021/acscentsci.7b00338
ACS Cent. Sci. 2017, 3, 1156−1167

have recently provided evidence that Fis1 is instead dispensable for mitochondrial membrane fission, supporting the notion that Dnm1/Drp1-mediated mitochondrial fission is not necessarily a conserved function of Fis1.[77] Furthermore, the human homologue hFis1 does not appear to recruit Drp1 to mitochondria.[83,84] Therefore, although Fis1 is a conserved factor for fission and believed to function with Dnm1, its specific role in mitochondrial fission is unclear. Using the same approach used for Dnm1, we examine Fis1 for possible membrane activity.

Fis1 Is Not Predicted To Contain Membrane-Destabilizing Sequences and Does Not Restructure Mitochondrial-like Membranes. Fis1 (~16 kDa) is a highly conserved tail-anchored protein in the mitochondrial outer membrane that is believed to be involved in mitochondrial fission with Dnm1. Fis1 has a cytosolic N-terminal domain that contains a six-helix array with two tandem tetratricopeptide repeat motifs (TPR) and a C-terminal transmembrane (TM) domain serving as an anchor into the mitochondrial outer membrane[18,85] (Figure 4A).

With the machine-learning classifier, we evaluated Fis1 for potential membrane-destabilizing helical sequences. We ran a moving window scan on the protein sequence (UniProtKB: P40515) for subsequences of 10−25 residues and compared the outputs with the determined protein crystal structure (PDB: 3O48).[86] While the algorithm predicted a few helical sequences to have a positive σ score, none were identified with a high probability ($P(+1) > 0.95$) for membrane activity (Figure 4B). Overall, these results indicate that Fis1 is unlikely to be membrane-destabilizing or have a direct role in the membrane restructuring that occurs during mitochondrial fission.

Using SAXS, we examined SUVs incubated with Fis1 at a P/L molar ratio of 1/500 and indeed found that the protein did not restructure the lipid vesicles. Instead, the SAXS profile for each model membrane, 75/15/10 and 75/5/20 PE/PC/CL (Figure 4C), exhibited a broad feature that is consistent with the form factor of unilamellar vesicles and resembled the spectra observed for the control SUVs (Figure S2). More specifically, Fis1 does not generate NGC and, therefore, would not be expected to have direct membrane activity that mediates membrane fission in the manner of Dnm1, which is consistent with our machine-learning predictions.

Fis1 Inhibits Dnm1-Mediated Membrane Disruption. That Fis1 does not restructure membranes in the manner of Dnm1, by inducing NGC, raises interesting questions on precisely what its physical role is, given extant results on its unambiguous contributions to the fission process. To expand on the observation that Fis1 does not disrupt model mitochondrial membranes by generating NGC, we investigate how Fis1 interacts with Dnm1, and do so in the context of membrane interactions, since direct interactions between Dnm1 and Fis1 have been previously studied.[18,68,73] Specifically, we explored how Dnm1 in combination with Fis1 impacts Dnm1 membrane remodeling.

SUVs were incubated with both Dnm1 (P/L = 1/1000) and Fis1 (P/L = 1/500) and measured using SAXS. Model membrane 75/15/10 PE/PC/CL exhibited an H_{II} phase with a lattice parameter of 7.94 nm, while membrane 75/5/20 PE/PC/CL possessed an H_{II} phase and a coexistence of *Im*3*m* and *Pn*3*m* Q_{II} phases, characterized by lattice parameters of 7.83, 24.09, and 19.00 nm, respectively (Figure 5). Comparing these SAXS measurements to our previous results, we noted changes

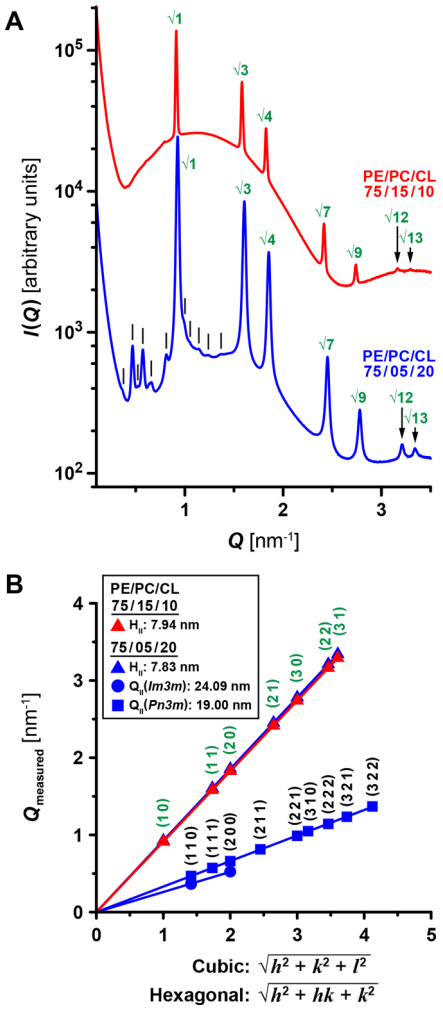

Figure 5. Dnm1 exhibits reduced ability to generate NGC in the presence of Fis1. (A) Dnm1 (P/L = 1/1000) in combination with Fis1 (P/L = 1/500) restructured both 75/15/10 and 75/5/20 PE/PC/CL model membranes but with decreased membrane curvature induction compared to Dnm1 alone (Figure 2). Correlation peaks corresponding to assigned reflections are indicated for hexagonal (green) and cubic (black lines) phases. (B) Indexing of generated H_{II}, and *Im*3*m* and *Pn*3*m* Q_{II} phases for 75/15/10 (red) and 75/5/20 (blue) PE/PC/CL membranes reveals increases in the lattice parameters for all induced phases compared to membranes incubated only with Dnm1 (Figure 2C). These larger lattice parameters and no observed *Pn*3*m* Q_{II} phase for 75/15/10 PE/PC/CL indicate a marked attenuation in overall curvature induction and a reduced ability of Dnm1 to generate NGC.

in the phase identity and magnitude of membrane curvature induced by Dnm1 while in the presence of Fis1. Specifically, for membrane 75/15/10 PE/PC/CL, the *Pn*3*m* Q_{II} phase induced by Dnm1 alone (Figure 2A,C) is now no longer apparent (Figure 5). Similarly, the *Im*3*m* Q_{II} phase that resulted from MBP-Dnm1 alone is also now absent (Figure S3). These disappearances of cubic phases imply a marked reduction in the ability of Dnm1 to generate NGC in mitochondrial-like membranes while in the presence of Fis1. Furthermore, we found that the lattice parameter of the hexagonal phase increased from 7.88 to 7.94 nm. Larger lattices were also observed for all coexisting phases in model membrane 75/5/20 PE/PC/CL, with unit-cell spacing increasing from 7.70 to 7.83 nm (H_{II}), 20.65 to 24.09 nm (*Im*3*m* Q_{II}), and 16.15 to 19.00 nm (*Pn*3*m* Q_{II}). Importantly, these increased lattice parameters

DOI: 10.1021/acscentsci.7b00338
ACS Cent. Sci. 2017, 3, 1156−1167

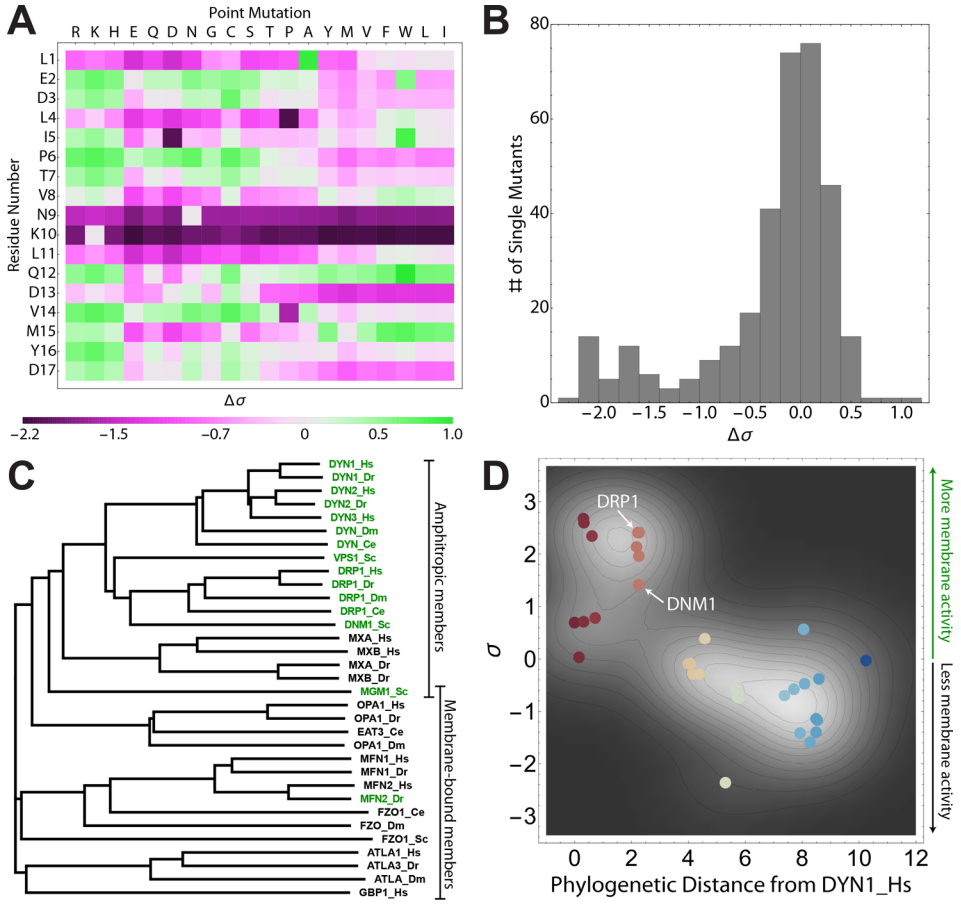

Figure 6. Membrane activity fitness landscape of the Dnm1 N-terminal helix and evolution of membrane activity in the dynamin superfamily. (A) 2D heat map of the membrane activity fitness landscape of the Dnm1 N-terminal helix. Fitness of 323 unique single mutants is calculated as $\Delta\sigma = \sigma_{mutant} - \sigma_{WT}$. Mutations predicted to reduce membrane activity are shown in magenta, while those that conserve membrane activity are shown in green. (B) Distribution of $\Delta\sigma$ shows that the mutational landscape is skewed toward reduced σ (negative $\Delta\sigma$), indicating that the Dnm1 N-terminal helix is well-optimized for membrane activity. (C) A phylogram is constructed via multiple sequence alignment of 33 dynamin superfamily members, including yeast Dnm1 (DNM1_Sc) and human Drp1 (DRP1_Hs) (Figure S5). The lengths of the branches are proportional to the phylogenetic distance from the nearest ancestral branch. Machine-learning screens for membrane activity were carried out on an aligned 16-amino-acid span corresponding to the conserved N-terminal helix in Dnm1 and Drp1. The members shown in green are predicted to be able to generate NGC ($\sigma > 0$), while those in black are not ($\sigma < 0$). All family members shown in green except for MFN2_Dr are amphitropic (lacking a TM domain), while most family members shown in black contain TM domains (except for MXA_Hs, MXB_Hs, MXA_Dr, and MXB_Dr). (D) Phylogenetic distance from the reference human dynamin DYN1_Hs is inversely related to the predicted ability to generate NGC (σ). Dynamin family members are color coded by phylogenetic distance, in units of number of substitutions per site (red = closet, blue = furthest). As phylogenetic distance increases, ability to generate NGC is decreased ($R_{Pearson} = -0.728$ [−0.859, −0.587], $P < 10^{-5}$, $R_{Spearman} = -0.750$ [−0.863, −0.560], $P < 10^{-5}$, $N = 33$). The density plot shows two clusters of sequences, with the upper left cluster roughly corresponding to the amphitropic members and the lower right cluster roughly corresponding to the membrane-tethered members. The locations of DNM1_Sc and DRP1_Hs are labeled in white. Raw data are found in Table S1.

correspond to decreased magnitudes of induced membrane curvature for each associated phase, as the two characteristics are inversely related.[71,87,88] For instance, while a hexagonal phase is characterized by having a Gaussian curvature of zero, it has a mean curvature of $H \approx -1/a$ (radius of hexagonal lipid cylinder $\approx 0.5a$), and cubic phases have an average Gaussian curvature of $\langle K \rangle = (2\pi\chi)/(A_0 a^2)$. Both of these quantities decrease in magnitude with an increasing lattice parameter a. Specifically, the increased lattice parameters for the *Im*3*m* and *Pn*3*m* cubic phases correspond quantitatively to a decrease in NGC magnitude from $\langle K \rangle = -2.5 \times 10^{-2}$ nm^{-2} for Dnm1 alone to $\langle K \rangle = -1.8 \times 10^{-2}$ nm^{-2} for Dnm1 in the presence of Fis1. These findings indicate that Fis1 limits the ability of Dnm1 to generate membrane curvature that would facilitate mitochondrial fission. That the interactions between Fis1 and Dnm1 are complex from extant studies suggests that the action of Fis1 in this context may be pleiotropic, impacting Dnm1 through multiple channels of activity such as protein−protein binding or direct induction of complementary membrane curvature to "cancel" NGC. Yeast cell biological findings are congruent with this idea in that Fis1 may act at two distinct stages in fission.[68,89] Thus, the combined membrane activity of Dnm1 and Fis1 in principle affords the ability to control the equilibrium diameter of the fission neck, in a way that is complementary to the mechanical constriction model.

Membrane Activity Fitness Landscape of the Dnm1 N-Terminal Helix and Evolution of Membrane Activity in the Dynamin Superfamily. Now that we have experimentally validated the ability of Dnm1 to directly generate NGC in mitochondrial-like membranes, we apply the machine-learning classifier to explore the membrane activity fitness landscape of the Dnm1 N-terminal helix, and trace the evolution of the

DOI: 10.1021/acscentsci.7b00338
ACS Cent. Sci. 2017, 3, 1156−1167

membrane-remodeling ability of this helical domain in members of the dynamin protein superfamily. In our previous work, we combined machine learning with experimental SAXS measurements to demonstrate that a positive, monotonic relationship exists between σ and the NGC-generating ability of membrane-active helical peptides.[41] Conveniently, the observed NGC induced by Dnm1 (-2.5×10^{-2} nm^{-2}) and its σ score (1.36) fall exactly within the predictive range established by previous SAXS experiments. This relationship thus allows us to evaluate the local membrane activity fitness landscape of Dnm1 and its related family members without the cost of experimentally screening hundreds of mutants (this strategy has been previously used in the context of protein stability and viral fitness[90,91]).

First, we conducted an *in silico* mutational analysis of the N-terminal helical sequence corresponding to the top hit from the initial machine-learning screen (LEDLIPTVNKLQDVMYD, Figure 1A,B). 323 unique single mutants (17 × 19) were generated and screened using the SVM-based membrane activity classifier.[41] The σ values of all single mutants were quantitatively compared to the wild type (WT) sequence by the metric $\Delta\sigma = \sigma_{mutant} - \sigma_{WT}$. An increase in σ upon mutation ($\Delta\sigma > 0$) corresponded to conservation of NGC-generating activity, and a decrease in σ upon mutation ($\Delta\sigma < 0$) predicted a loss of NGC-generating activity. The sign and magnitude of $\Delta\sigma$ for each single mutant is plotted on a heat map (Figure 6A), and the distribution of $\Delta\sigma$ is quantified (Figure 6B). Interestingly, residues N9 and K10 were found to be especially important for membrane activity, with all 19 possible mutations leading to large reductions in σ. Other important residues include L1, L4, L11, D13, and D17 (Figure S4). This demonstrates that the majority of single mutations led to reductions in σ and the predicted ability to generate NGC. The average value of $\Delta\sigma$ for all single mutants was −0.29, and the distribution of $\Delta\sigma$ values is heavily skewed to negative values (skewness = −1.43) (Figure 6B). In fact, a third of the single mutants (108) led to drastic reductions in σ ($\Delta\sigma \leq -0.3$). Overall, this mutational analysis of the Dnm1 N-terminal helix demonstrates that the WT sequence is well-optimized for membrane-restructuring activity.

Next, to examine the membrane activity of Dnm1 in the global scope of dynamin superfamily proteins, we conducted machine-learning screens on the homologous helical domains of family members. A sequence alignment (Figure S5) and phylogenetic reconstruction of 33 members of the dynamin superfamily from various organisms (Figure 6C) revealed that dynamins fall into two previously unrecognized groups: membrane-bound (containing a TM domain) and amphitropic, which are freely soluble proteins that reversibly interact with membranes (lacking a TM domain). We calculated σ for the homologous segments of the 33 dynamin superfamily members (Table S1) and found that 15 of the sequences were predicted to have NGC-generating activity ($\sigma > 0$) while 18 did not ($\sigma < 0$) (Figure 6C,D). Based on sequence alignment and secondary structure prediction, these conserved regions are likely helical. While 14 of the 15 positive hits belonged to amphitropic dynamins, 14 of the 18 proteins that were predicted to lack NGC-generating domains belonged to the membrane-tethered dynamins (MGM1_Sc is a member of both families since it has a long membrane-bound form and a short amphitropic form[92]). Based on this finding, we hypothesized that amphitropic dynamin superfamily members evolved the ability to generate NGC to augment their membrane-remodeling functions. To probe the quantitative relationship between the ability to generate NGC and the evolutionary history of dynamin-related proteins, we calculated the strength of correlation between σ and the phylogenetic distance of each family member from the human classical dynamin DYN1_Hs (Figure 6D). We calculated Pearson and Spearman correlations, as well as the newly developed nonlinear correlation metrics distance correlation (dCor)[93] and maximal information coefficient (MIC).[94] Surprisingly, we find a strong, statistically significant negative correlation between phylogenetic distance and predicted ability to generate NGC (σ) ($R_{Pearson} = -0.728$ [−0.859, −0.587], $P < 10^{-5}$; $R_{Spearman} = -0.750$ [−0.863, −0.560], $P < 10^{-5}$). Nonlinear correlations suggest a strong statistical dependence between σ and phylogenetic distance ($R_{dCor} = 0.781$ [0.678, 0.883], $P < 10^{-5}$; $R_{MIC} = 0.832$ [0.786, 0.999], $P < 10^{-5}$). Indeed, these results suggest that amphitropic members of the dynamin superfamily evolved the ability to generate NGC, and the predicted strength of NGC generation scales inversely with evolutionary distance. A density analysis of σ versus phylogenetic distance reveals two clusters of dynamin superfamily members, which closely recapitulates the classification of the proteins as amphitropic (Figure 6D, upper left) and membrane-tethered (Figure 6D, lower right).

CONCLUSIONS AND PROSPECTS

In summary, results from machine learning and synchrotron SAXS indicate that the fission protein Dnm1 may catalyze mitochondrial fission by both its GTPase hydrolysis-driven mitochondrial mechanical pinching activity and its synergistic membrane-remodeling activity. The observations here provide a framework to reconcile diverse extant results. The NGC thus generated by Dnm1 can reach fission neck sizes of 12.6 nm in diameter, which is smaller than the observed diameters of ∼120 nm and ∼70 nm, in the absence and presence of nucleotide, respectively, from mechanical constriction,[24,27] suggesting that membrane remodeling may amplify effects from motor activity alone. The existence of strong membrane-remodeling activity provides a point of contact with recently observed roles for specific membrane lipids in mitochondrial fission: The ability of Dnm1 to form oligomeric spirals and induce NGC suggests that the protein drives mitochondrial membrane constriction through a combination of both mechanical pinching effects and membrane remodeling by creating the curvature needed for scission neck formation. We note that it is possible that the two effects are synergistic, since mechanical constriction can locally enrich negative spontaneous curvature PE lipids in the neck region,[95] which will in turn lower the absolute value of the Gaussian modulus and thereby make it even easier to form narrower necks.[56] Finally, that the sequence domain for membrane curvature generation falls within a highly conserved region between Dnm1 and Drp1 suggests that such membrane activity may be a general feature of dynamin superfamily GTPases.[96]

The findings presented here also suggest that Fis1 may regulate the ability of Dnm1 to induce membrane-destabilizing curvature that would promote mitochondrial fission. Indeed, our measurements demonstrate that Fis1 alone does not disrupt bilayer membranes at the stoichiometries examined. However, it is possible that the protein induces membrane curvature that counteracts the NGC-inducing activity of Dnm1. In support of this notion, previous studies have demonstrated that Fis1 binds directly with membranes and that this

DOI: 10.1021/acscentsci.7b00338
ACS Cent. Sci. 2017, 3, 1156−1167

interaction can lead to vesicle clustering that is not membrane-disruptive, as the vesicles retain their original shape.[97] Previous experiments on yeast cells have also shown that Dnm1-mediated mitochondrial fission can be inhibited by Fis1.[98] However, the landscape of interactions is likely complex, given that expression of Fis1 and Dnm1 alone is insufficient for fission,[20,77] which can occur upon expression of the adaptor Mdv1.[20,72,77] Based on these results, we hypothesize that the regulation of Dnm1 activity by Fis1, as an inhibitor, may play a role in regulating mitochondrial fission by controlling the effective diameter of the fission neck in a parallel channel of activity in addition to mechanoconstriction.

METHODS

Dnm1 and Fis1 proteins were expressed and purified as previously described.[99] We used a previously published SVM-based machine-learning tool[41] in conjunction with sequence alignment, homology modeling, and secondary structure prediction to screen for membrane-active sequences. Proteins were incubated with model mitochondrial membranes and characterized with SAXS. A phylogenetic reconstruction of 33 dynamin superfamily members was generated, and aligned sequences were screened for membrane activity.

Further details can be found in the Supporting Information.

ASSOCIATED CONTENT

Supporting Information

The Supporting Information is available free of charge on the ACS Publications website at DOI: 10.1021/acscentsci.7b00338.

Methods, sequence alignments, SAXS spectra, sequence mutability analysis, machine-learning screen outputs, phylogenetic analysis (PDF)

AUTHOR INFORMATION

Corresponding Authors

*E-mail: gclwong@seas.ucla.edu.

*E-mail: rbhill@mcw.edu.

ORCID

Michelle W. Lee: 0000-0003-1613-9501

Ernest Y. Lee: 0000-0001-5144-2552

Ghee Hwee Lai: 0000-0002-3310-3992

Ammon E. Posey: 0000-0002-1445-6522

Wujing Xian: 0000-0001-5074-0304

Andrew L. Ferguson: 0000-0002-8829-9726

R. Blake Hill: 0000-0001-6228-3905

Present Address

‡G.H.L.: Singapore Centre for Environmental Life Sciences Engineering (SCELSE), Singapore.

Notes

The authors declare no competing financial interest.

ACKNOWLEDGMENTS

We thank Dr. Jeffery F. Miller for helpful discussions regarding the phylogenetic analysis. This work is supported by grants from the National Science Foundation (DMR-1411329 to G.C.L.W.) and the National Institutes of Health (R01GM067180 to R.B.H.) Use of the Stanford Synchrotron Radiation Lightsource, SLAC National Accelerator Laboratory, is supported by the U.S. Department of Energy, Office of Science, Office of Basic Energy Sciences, under Contract No. DE-AC02-76SF00515. The SSRL Structural Molecular Biology Program is supported by the DOE Office of Biological and Environmental Research and by the National Institutes of Health, National Institute of General Medical Sciences (including P41GM103393).

REFERENCES

(1) Youle, R. J.; van der Bliek, A. M. Mitochondrial Fission, Fusion, and Stress. *Science* **2012**, *337*, 1062−1065.

(2) Otera, H.; Ishihara, N.; Mihara, K. New Insights Into the Function and Regulation of Mitochondrial Fission. *Biochim. Biophys. Acta, Mol. Cell Res.* **2013**, *1833*, 1256−1268.

(3) Chang, D. T. W.; Honick, A. S.; Reynolds, I. J. Mitochondrial Trafficking to Synapses in Cultured Primary Cortical Neurons. *J. Neurosci.* **2006**, *26*, 7035−7045.

(4) Saxton, W. M.; Hollenbeck, P. J. The Axonal Transport of Mitochondria. *J. Cell Sci.* **2012**, *125*, 2095−2104.

(5) Li, Z.; Okamoto, K.-I.; Hayashi, Y.; Sheng, M. The Importance of Dendritic Mitochondria in the Morphogenesis and Plasticity of Spines and Synapses. *Cell* **2004**, *119*, 873−887.

(6) Shaw, J. M.; Nunnari, J. Mitochondrial Dynamics and Division in Budding Yeast. *Trends Cell Biol.* **2002**, *12*, 178−184.

(7) Westermann, B. Mitochondrial Fusion and Fission in Cell Life and Death. *Nat. Rev. Mol. Cell Biol.* **2010**, *11*, 872−884.

(8) Sesaki, H.; Jensen, R. E. Division Versus Fusion: Dnm1p and Fzo1p Antagonistically Regulate Mitochondrial Shape. *J. Cell Biol.* **1999**, *147*, 699−706.

(9) Bleazard, W.; McCaffery, J. M.; King, E. J.; Bale, S.; Mozdy, A.; Tieu, Q.; Nunnari, J.; Shaw, J. M. The Dynamin-Related GTPase Dnm1 Regulates Mitochondrial Fission in Yeast. *Nat. Cell Biol.* **1999**, *1*, 298−304.

(10) Smirnova, E.; Shurland, D. L.; Ryazantsev, S. N.; van der Bliek, A. M. A Human Dynamin-Related Protein Controls the Distribution of Mitochondria. *J. Cell Biol.* **1998**, *143*, 351−358.

(11) Otsuga, D.; Keegan, B. R.; Brisch, E.; Thatcher, J. W.; Hermann, G. J.; Bleazard, W.; Shaw, J. M. The Dynamin-Related GTPase, Dnm1p, Controls Mitochondrial Morphology in Yeast. *J. Cell Biol.* **1998**, *143*, 333−349.

(12) Chan, D. C. Mitochondrial Fusion and Fission in Mammals. *Annu. Rev. Cell Dev. Biol.* **2006**, *22*, 79−99.

(13) Itoh, K.; Nakamura, K.; Iijima, M.; Sesaki, H. Mitochondrial Dynamics in Neurodegeneration. *Trends Cell Biol.* **2013**, *23*, 64−71.

(14) Knott, A. B.; Perkins, G.; Schwarzenbacher, R.; Bossy-Wetzel, E. Mitochondrial Fragmentation in Neurodegeneration. *Nat. Rev. Neurosci.* **2008**, *9*, 505−518.

(15) Mozdy, A. D.; McCaffery, J. M.; Shaw, J. M. Dnm1p GTPase-Mediated Mitochondrial Fission Is a Multi-Step Process Requiring the Novel Integral Membrane Component Fis1p. *J. Cell Biol.* **2000**, *151*, 367−379.

(16) James, D. I.; Parone, P. A.; Mattenberger, Y.; Martinou, J.-C. hFis1, a Novel Component of the Mammalian Mitochondrial Fission Machinery. *J. Biol. Chem.* **2003**, *278*, 36373−36379.

(17) Smirnova, E.; Griparic, L.; Shurland, D. L.; van der Bliek, A. M. Dynamin-Related Protein Drp1 Is Required for Mitochondrial Division in Mammalian Cells. *Mol. Biol. Cell* **2001**, *12*, 2245−2256.

(18) Yoon, Y.; Krueger, E. W.; Oswald, B. J.; McNiven, M. A. The Mitochondrial Protein hFis1 Regulates Mitochondrial Fission in Mammalian Cells Through an Interaction with the Dynamin-Like Protein DLP1. *Mol. Cell. Biol.* **2003**, *23*, 5409−5420.

(19) Stojanovski, D.; Koutsopoulos, O. S.; Okamoto, K.; Ryan, M. T. Levels of Human Fis1 at the Mitochondrial Outer Membrane Regulate Mitochondrial Morphology. *J. Cell Sci.* **2004**, *117*, 1201−1210.

(20) Tieu, Q.; Nunnari, J. Mdv1p Is a WD Repeat Protein That Interacts with the Dynamin-Related GTPase, Dnm1p, to Trigger Mitochondrial Division. *J. Cell Biol.* **2000**, *151*, 353−365.

(21) Labrousse, A. M.; Zappaterra, M. D.; Rube, D. A.; van der Bliek, A. M. C-Elegans Dynamin-Related Protein DRP-1 Controls Severing of the Mitochondrial Outer Membrane. *Mol. Cell* **1999**, *4*, 815−826.

DOI: 10.1021/acscentsci.7b00338
ACS Cent. Sci. 2017, 3, 1156−1167

(22) Fukushima, N. H.; Brisch, E.; Keegan, B. R.; Bleazard, W.; Shaw, J. M. The GTPase Effector Domain Sequence of the Dnm1p GTPase Regulates Self-Assembly and Controls a Rate-Limiting Step in Mitochondrial Fission. *Mol. Biol. Cell* **2001**, *12*, 2756−2766.
(23) Sesaki, H.; Adachi, Y.; Kageyama, Y.; Itoh, K.; Iijima, M. In Vivo Functions of Drp1: Lessons Learned From Yeast Genetics and Mouse Knockouts. *Biochim. Biophys. Acta, Mol. Basis Dis.* **2014**, *1842*, 1179−1185.
(24) Ingerman, E.; Perkins, E. M.; Marino, M.; Mears, J. A.; McCaffery, J. M.; Hinshaw, J. E.; Nunnari, J. Dnm1 Forms Spirals That Are Structurally Tailored to Fit Mitochondria. *J. Cell Biol.* **2005**, *170*, 1021−1027.
(25) Lackner, L. L.; Horner, J. S.; Nunnari, J. Mechanistic Analysis of a Dynamin Effector. *Science* **2009**, *325*, 874−877.
(26) Bhar, D.; Karren, M. A.; Babst, M.; Shaw, J. M. Dimeric Dnm1-G385D Interacts with Mdv1 on Mitochondria and Can Be Stimulated to Assemble Into Fission Complexes Containing Mdv1 and Fis1. *J. Biol. Chem.* **2006**, *281*, 17312−17320.
(27) Mears, J. A.; Lackner, L. L.; Fang, S.; Ingerman, E.; Nunnari, J.; Hinshaw, J. E. Conformational Changes in Dnm1 Support a Contractile Mechanism for Mitochondrial Fission. *Nat. Struct. Mol. Biol.* **2011**, *18*, 20−26.
(28) Daumke, O.; Praefcke, G. J. K. Invited Review: Mechanisms of GTP Hydrolysis and Conformational Transitions in the Dynamin Superfamily. *Biopolymers* **2016**, *105*, 580−593.
(29) Stepanyants, N.; Macdonald, P. J.; Francy, C. A.; Mears, J. A.; Qi, X.; Ramachandran, R. Cardiolipin's Propensity for Phase Transition and Its Reorganization by Dynamin-Related Protein 1 Form a Basis for Mitochondrial Membrane Fission. *Mol. Biol. Cell* **2015**, *26*, 3104−3116.
(30) Frohman, M. A. Role of Mitochondrial Lipids in Guiding Fission and Fusion. *J. Mol. Med.* **2015**, *93*, 263−269.
(31) Ugarte-Uribe, B.; Müller, H.-M.; Otsuki, M.; Nickel, W.; García-Sáez, A. J. Dynamin-Related Protein 1 (Drp1) Promotes Structural Intermediates of Membrane Division. *J. Biol. Chem.* **2014**, *289*, 30645−30656.
(32) Morlot, S.; Roux, A. Mechanics of Dynamin-Mediated Membrane Fission. *Annu. Rev. Biophys.* **2013**, *42*, 629−649.
(33) Shnyrova, A. V.; Bashkirov, P. V.; Akimov, S. A.; Pucadyil, T. J.; Zimmerberg, J.; Schmid, S. L.; Frolov, V. A. Geometric Catalysis of Membrane Fission Driven by Flexible Dynamin Rings. *Science* **2013**, *339*, 1433−1436.
(34) Montessuit, S.; Somasekharan, S. P.; Terrones, O.; Lucken-Ardjomande, S.; Herzig, S.; Schwarzenbacher, R.; Manstein, D. J.; Bossy-Wetzel, E.; Basañez, G.; Meda, P.; et al. Membrane Remodeling Induced by the Dynamin-Related Protein Drp1 Stimulates Bax Oligomerization. *Cell* **2010**, *142*, 889−901.
(35) Macdonald, P. J.; Stepanyants, N.; Mehrotra, N.; Mears, J. A.; Qi, X.; Sesaki, H.; Ramachandran, R. A Dimeric Equilibrium Intermediate Nucleates Drp1 Reassembly on Mitochondrial Membranes for Fission. *Mol. Biol. Cell* **2014**, *25*, 1905−1915.
(36) Heymann, J. A. W.; Hinshaw, J. E. Dynamins at a Glance. *J. Cell Sci.* **2009**, *122*, 3427−3431.
(37) Francy, C. A.; Clinton, R. W.; Fröhlich, C.; Murphy, C.; Mears, J. A. Cryo-EM Studies of Drp1 Reveal Cardiolipin Interactions That Activate the Helical Oligomer. *Sci. Rep.* **2017**, *7*, R283.
(38) Stachowiak, J. C.; Schmid, E. M.; Ryan, C. J.; Ann, H. S.; Sasaki, D. Y.; Sherman, M. B.; Geissler, P. L.; Fletcher, D. A.; Hayden, C. C. Membrane Bending by Protein−Protein Crowding. *Nat. Cell Biol.* **2012**, *14*, 944−949.
(39) Stachowiak, J. C.; Hayden, C. C.; Sasaki, D. Y. Steric Confinement of Proteins on Lipid Membranes Can Drive Curvature and Tubulation. *Proc. Natl. Acad. Sci. U. S. A.* **2010**, *107*, 7781−7786.
(40) Snead, W. T.; Hayden, C. C.; Gadok, A. K.; Zhao, C.; Lafer, E. M.; Rangamani, P.; Stachowiak, J. C. Membrane Fission by Protein Crowding. *Proc. Natl. Acad. Sci. U. S. A.* **2017**, *114*, E3258−E3267.
(41) Lee, E. Y.; Fulan, B. M.; Wong, G. C. L.; Ferguson, A. L. Mapping Membrane Activity in Undiscovered Peptide Sequence Space Using Machine Learning. *Proc. Natl. Acad. Sci. U. S. A.* **2016**, *113*, 13588−13593.
(42) Schmidt, N. W.; Mishra, A.; Lai, G. H.; Davis, M.; Sanders, L. K.; Tran, D.; Garcia, A.; Tai, K. P.; McCray, P. B.; Ouellette, A. J.; et al. Criterion for Amino Acid Composition of Defensins and Antimicrobial Peptides Based on Geometry of Membrane Destabilization. *J. Am. Chem. Soc.* **2011**, *133*, 6720−6727.
(43) Schmidt, N. W.; Mishra, A.; Lai, G. H.; Wong, G. C. L. Arginine-Rich Cell-Penetrating Peptides. *FEBS Lett.* **2010**, *584*, 1806−1813.
(44) Gelbart, W. M.; Ben-Shaul, A.; Roux, D. D. *Micelles, Membranes, Microemulsions, and Monolayers*; Springer-Verlag: New York, 1994.
(45) Gómez-Llobregat, J.; Elías-Wolff, F.; Lindén, M. Anisotropic Membrane Curvature Sensing by Amphipathic Peptides. *Biophys. J.* **2016**, *110*, 197−204.
(46) Lear, J. D.; DeGrado, W. F. Membrane Binding and Conformational Properties of Peptides Representing the NH2 Terminus of Influenza HA-2. *J. Biol. Chem.* **1987**, *262*, 6500−6505.
(47) Wenzel, M.; Chiriac, A. I.; Otto, A.; Zweytick, D.; May, C.; Schumacher, C.; Gust, R.; Albada, H. B.; Penkova, M.; Krämer, U.; et al. Small Cationic Antimicrobial Peptides Delocalize Peripheral Membrane Proteins. *Proc. Natl. Acad. Sci. U. S. A.* **2014**, *111*, E1409−E1418.
(48) Sato, H.; Feix, J. B. Peptide-Membrane Interactions and Mechanisms of Membrane Destruction by Amphipathic Alpha-Helical Antimicrobial Peptides. *Biochim. Biophys. Acta, Biomembr.* **2006**, *1758*, 1245−1256.
(49) Makovitzki, A.; Avrahami, D.; Shai, Y. Ultrashort Antibacterial and Antifungal Lipopeptides. *Proc. Natl. Acad. Sci. U. S. A.* **2006**, *103*, 15997−16002.
(50) Lorizate, M.; Huarte, N.; Sáez-Cirión, A.; Nieva, J. L. Interfacial Pre-Transmembrane Domains in Viral Proteins Promoting Membrane Fusion and Fission. *Biochim. Biophys. Acta, Biomembr.* **2008**, *1778*, 1624−1639.
(51) Epand, R. M. Fusion Peptides and the Mechanism of Viral Fusion. *Biochim. Biophys. Acta, Biomembr.* **2003**, *1614*, 116−121.
(52) Schmidt, N. W.; Wong, G. C. L. Antimicrobial Peptides and Induced Membrane Curvature: Geometry, Coordination Chemistry, and Molecular Engineering. *Curr. Opin. Solid State Mater. Sci.* **2013**, *17*, 151−163.
(53) Schmidt, N. W.; Tai, K. P.; Kamdar, K.; Mishra, A.; Lai, G. H.; Zhao, K.; Ouellette, A. J.; Wong, G. C. L. Arginine in A-Defensins: Differential Effects on Bactericidal Activity Correspond to Geometry of Membrane Curvature Generation and Peptide-Lipid Phase Behavior. *J. Biol. Chem.* **2012**, *287*, 21866−21872.
(54) Hu, K.; Schmidt, N. W.; Zhu, R.; Jiang, Y.; Lai, G. H.; Wei, G.; Palermo, E. F.; Kuroda, K.; Wong, G. C. L.; Yang, L. A Critical Evaluation of Random Copolymer Mimesis of Homogeneous Antimicrobial Peptides. *Macromolecules* **2013**, *46*, 1908−1915.
(55) Lee, M. W.; Chakraborty, S.; Schmidt, N. W.; Murgai, R.; Gellman, S. H.; Wong, G. C. L. Two Interdependent Mechanisms of Antimicrobial Activity Allow for Efficient Killing in Nylon-3-Based Polymeric Mimics of Innate Immunity Peptides. *Biochim. Biophys. Acta, Biomembr.* **2014**, *1838*, 2269−2279.
(56) Yang, L.; Gordon, V. D.; Trinkle, D. R.; Schmidt, N. W.; Davis, M. A.; DeVries, C.; Som, A.; Cronan, J. E. J.; Tew, G. N.; Wong, G. C. L. Mechanism of a Prototypical Synthetic Membrane-Active Antimicrobial: Efficient Hole-Punching via Interaction with Negative Intrinsic Curvature Lipids. *Proc. Natl. Acad. Sci. U. S. A.* **2008**, *105*, 20595−20600.
(57) Schmidt, N. W.; Lis, M.; Zhao, K.; Lai, G. H.; Alexandrova, A. N.; Tew, G. N.; Wong, G. C. L. Molecular Basis for Nanoscopic Membrane Curvature Generation From Quantum Mechanical Models and Synthetic Transporter Sequences. *J. Am. Chem. Soc.* **2012**, *134*, 19207−19216.
(58) Mishra, A.; Lai, G. H.; Schmidt, N. W.; Sun, V. Z.; Rodriguez, A. R.; Tong, R.; Tang, L.; Cheng, J.; Deming, T. J.; Kamei, D. T.; et al. Translocation of HIV TAT Peptide and Analogues Induced by Multiplexed Membrane and Cytoskeletal Interactions. *Proc. Natl. Acad. Sci. U. S. A.* **2011**, *108*, 16883−16888.

DOI: 10.1021/acscentsci.7b00338
ACS Cent. Sci. 2017, 3, 1156−1167

(59) Mishra, A.; Gordon, V. D.; Yang, L.; Coridan, R.; Wong, G. C. L. HIV TAT Forms Pores in Membranes by Inducing Saddle-Splay Curvature: Potential Role of Bidentate Hydrogen Bonding. *Angew. Chem., Int. Ed.* **2008**, *47*, 2986−2989.
(60) Yao, H.; Lee, M. W.; Waring, A. J.; Wong, G. C. L.; Hong, M. Viral Fusion Protein Transmembrane Domain Adopts B-Strand Structure to Facilitate Membrane Topological Changes for Virus-Cell Fusion. *Proc. Natl. Acad. Sci. U. S. A.* **2015**, *112*, 10926−10931.
(61) Schmidt, N. W.; Mishra, A.; Wang, J.; DeGrado, W. F.; Wong, G. C. L. Influenza Virus a M2 Protein Generates Negative Gaussian Membrane Curvature Necessary for Budding and Scission. *J. Am. Chem. Soc.* **2013**, *135*, 13710−13719.
(62) Lee, E. Y.; Wong, G. C. L.; Ferguson, A. L. Machine Learning-Enabled Discovery and Design of Membrane-Active Peptides. *Bioorg. Med. Chem.* **2017**, DOI: 10.1016/j.bmc.2017.07.012.
(63) Kabsch, W.; Sander, C. Dictionary of Protein Secondary Structure: Pattern Recognition of Hydrogen-Bonded and Geometrical Features. *Biopolymers* **1983**, *22*, 2577−2637.
(64) Fröhlich, C.; Grabiger, S.; Schwefel, D.; Faelber, K.; Rosenbaum, E.; Mears, J.; Rocks, O.; Daumke, O. Structural Insights Into Oligomerization and Mitochondrial Remodelling of Dynamin 1-Like Protein. *EMBO J.* **2013**, *32*, 1280−1292.
(65) Daum, G. Lipids of Mitochondria. *Biochim. Biophys. Acta, Rev. Biomembr.* **1985**, *822*, 1−42.
(66) Horvath, S. E.; Daum, G. Lipids of Mitochondria. *Prog. Lipid Res.* **2013**, *52*, 590−614.
(67) Ardail, D.; Privat, J. P.; Egret-Charlier, M.; Levrat, C.; Lerme, F.; Louisot, P. Mitochondrial Contact Sites. Lipid Composition and Dynamics. *J. Biol. Chem.* **1990**, *265*, 18797−18802.
(68) Koppenol-Raab, M.; Harwig, M. C.; Posey, A. E.; Egner, J. M.; MacKenzie, K. R.; Hill, R. B. A Targeted Mutation Identified Through pKa Measurements Indicates a Postrecruitment Role for Fis1 in Yeast Mitochondrial Fission. *J. Biol. Chem.* **2016**, *291*, 20329−20344.
(69) Chang, C.-R.; Manlandro, C. M.; Arnoult, D.; Stadler, J.; Posey, A. E.; Hill, R. B.; Blackstone, C. A Lethal De Novo Mutation in the Middle Domain of the Dynamin-Related GTPase Drp1 Impairs Higher Order Assembly and Mitochondrial Division. *J. Biol. Chem.* **2010**, *285*, 32494−32503.
(70) Francy, C. A.; Alvarez, F. J. D.; Zhou, L.; Ramachandran, R.; Mears, J. A. The Mechanoenzymatic Core of Dynamin-Related Protein 1 Comprises the Minimal Machinery Required for Membrane Constriction. *J. Biol. Chem.* **2015**, *290*, 11692−11703.
(71) Shearman, G. C.; Ces, O.; Templer, R. H.; Seddon, J. M. Inverse Lyotropic Phases of Lipids and Membrane Curvature. *J. Phys.: Condens. Matter* **2006**, *18*, S1105−S1124.
(72) Naylor, K.; Ingerman, E.; Okreglak, V.; Marino, M.; Hinshaw, J. E.; Nunnari, J. Mdv1 Interacts with Assembled Dnm1 to Promote Mitochondrial Division. *J. Biol. Chem.* **2006**, *281*, 2177−2183.
(73) Wells, R. C.; Picton, L. K.; Williams, S. C. P.; Tan, F. J.; Hill, R. B. Direct Binding of the Dynamin-Like GTPase, Dnm1, to Mitochondrial Dynamics Protein Fis1 Is Negatively Regulated by the Fis1 N-Terminal Arm. *J. Biol. Chem.* **2007**, *282*, 33769−33775.
(74) Kozlovsky, Y.; Kozlov, M. M. Membrane Fission: Model for Intermediate Structures. *Biophys. J.* **2003**, *85*, 85−96.
(75) Bui, H. T.; Shaw, J. M. Dynamin Assembly Strategies and Adaptor Proteins in Mitochondrial Fission. *Curr. Biol.* **2013**, *23*, R891−R899.
(76) Richter, V.; Singh, A. P.; Kvansakul, M.; Ryan, M. T.; Osellame, L. D. Splitting Up the Powerhouse: Structural Insights Into the Mechanism of Mitochondrial Fission. *Cell. Mol. Life Sci.* **2015**, *72*, 3695−3707.
(77) Koirala, S.; Guo, Q.; Kalia, R.; Bui, H. T.; Eckert, D. M.; Frost, A.; Shaw, J. M. Interchangeable Adaptors Regulate Mitochondrial Dynamin Assembly for Membrane Scission. *Proc. Natl. Acad. Sci. U. S. A.* **2013**, *110*, E1342−E1351.
(78) Yoon, Y.; Pitts, K. R.; McNiven, M. A. Mammalian Dynamin-Like Protein DLP1 Tubulates Membranes. *Mol. Biol. Cell* **2001**, *12*, 2894−2905.
(79) Lee, J. E.; Westrate, L. M.; Wu, H.; Page, C.; Voeltz, G. K. Multiple Dynamin Family Members Collaborate to Drive Mitochondrial Division. *Nature* **2016**, *540*, 139−143.
(80) Bustillo-Zabalbeitia, I.; Montessuit, S.; Raemy, E.; Basañez, G.; Terrones, O.; Martinou, J.-C. Specific Interaction with Cardiolipin Triggers Functional Activation of Dynamin-Related Protein 1. *PLoS One* **2014**, *9*, e102738.
(81) Macdonald, P. J.; Francy, C. A.; Stepanyants, N.; Lehman, L.; Baglio, A.; Mears, J. A.; Qi, X.; Ramachandran, R. Distinct Splice Variants of Dynamin-Related Protein 1 Differentially Utilize Mitochondrial Fission Factor as an Effector of Cooperative GTPase Activity. *J. Biol. Chem.* **2016**, *291*, 493−507.
(82) Cerveny, K. L.; Jensen, R. E. The WD-Repeats of Net2p Interact with Dnm1p and Fis1p to Regulate Division of Mitochondria. *Mol. Biol. Cell* **2003**, *14*, 4126−4139.
(83) Gandre-Babbe, S.; van der Bliek, A. M. The Novel Tail-Anchored Membrane Protein Mff Controls Mitochondrial and Peroxisomal Fission in Mammalian Cells. *Mol. Biol. Cell* **2008**, *19*, 2402−2412.
(84) Otera, H.; Wang, C.; Cleland, M. M.; Setoguchi, K.; Yokota, S.; Youle, R. J.; Mihara, K. Mff Is an Essential Factor for Mitochondrial Recruitment of Drp1 During Mitochondrial Fission in Mammalian Cells. *J. Cell Biol.* **2010**, *191*, 1141−1158.
(85) Suzuki, M.; Jeong, S.-Y.; Karbowski, M.; Youle, R. J.; Tjandra, N. The Solution Structure of Human Mitochondria Fission Protein Fis1 Reveals a Novel TPR-Like Helix Bundle. *J. Mol. Biol.* **2003**, *334*, 445−458.
(86) Tooley, J. E.; Khangulov, V.; Lees, J. P. B.; Schlessman, J. L.; Bewley, M. C.; Heroux, A.; Bosch, J.; Hill, R. B. The 1.75 Å Resolution Structure of Fission Protein Fis1 From Saccharomyces Cerevisiae Reveals Elusive Interactions of the Autoinhibitory Domain. *Acta Crystallogr., Sect. F: Struct. Biol. Cryst. Commun.* **2011**, *67*, 1310−1315.
(87) Seddon, J. M. Structure of the Inverted Hexagonal (Hii) Phase, and Non-Lamellar Phase-Transitions of Lipids. *Biochim. Biophys. Acta, Rev. Biomembr.* **1990**, *1031*, 1−69.
(88) Kozlov, M. M. Determination of Lipid Spontaneous Curvature From X-Ray Examinations of Inverted Hexagonal Phases. *Methods Mol. Biol.* **2007**, *400*, 355−366.
(89) Tieu, Q.; Okreglak, V.; Naylor, K.; Nunnari, J. The WD Repeat Protein, Mdv1p, Functions as a Molecular Adaptor by Interacting with Dnm1p and Fis1p During Mitochondrial Fission. *J. Cell Biol.* **2002**, *158*, 445−452.
(90) Ferguson, A. L.; Mann, J. K.; Omarjee, S.; Ndung'u, T.; Walker, B. D.; Chakraborty, A. K. Translating HIV Sequences Into Quantitative Fitness Landscapes Predicts Viral Vulnerabilities for Rational Immunogen Design. *Immunity* **2013**, *38*, 606−617.
(91) Romero, P. A.; Krause, A.; Arnold, F. H. Navigating the Protein Fitness Landscape with Gaussian Processes. *Proc. Natl. Acad. Sci. U. S. A.* **2013**, *110*, E193−E201.
(92) DeVay, R. M.; Dominguez-Ramirez, L.; Lackner, L. L.; Hoppins, S.; Stahlberg, H.; Nunnari, J. Coassembly of Mgm1 Isoforms Requires Cardiolipin and Mediates Mitochondrial Inner Membrane Fusion. *J. Cell Biol.* **2009**, *186*, 793−803.
(93) Székely, G. J.; Rizzo, M. L.; Bakirov, N. K. Measuring and Testing Dependence by Correlation of Distances. *Annals of Statistics* **2007**, *35*, 2769−2794.
(94) Reshef, D. N.; Reshef, Y. A.; Finucane, H. K.; Grossman, S. R.; McVean, G.; Turnbaugh, P. J.; Lander, E. S.; Mitzenmacher, M.; Sabeti, P. C. Detecting Novel Associations in Large Data Sets. *Science* **2011**, *334*, 1518−1524.
(95) Ostrowski, S. G.; Van Bell, C. T.; Winograd, N.; Ewing, A. G. Mass Spectrometric Imaging of Highly Curved Membranes During Tetrahymena Mating. *Science* **2004**, *305*, 71−73.
(96) Praefcke, G. J. K.; McMahon, H. T. The Dynamin Superfamily: Universal Membrane Tubulation and Fission Molecules? *Nat. Rev. Mol. Cell Biol.* **2004**, *5*, 133−147.
(97) Wells, R. C.; Hill, R. B. The Cytosolic Domain of Fis1 Binds and Reversibly Clusters Lipid Vesicles. *PLoS One* **2011**, *6*, e21384.

DOI: 10.1021/acscentsci.7b00338
ACS Cent. Sci. 2017, 3, 1156−1167

(98) Fannjiang, Y.; Cheng, W.-C.; Lee, S. J.; Qi, B.; Pevsner, J.; McCaffery, J. M.; Hill, R. B.; Basañez, G.; Hardwick, J. M. Mitochondrial Fission Proteins Regulate Programmed Cell Death in Yeast. *Genes Dev.* **2004**, *18*, 2785−2797.
(99) Picton, L. K.; Casares, S.; Monahan, A. C.; Majumdar, A.; Hill, R. B. Evidence for Conformational Heterogeneity of Fission Protein Fis1 From Saccharomyces Cerevisiae. *Biochemistry* **2009**, *48*, 6598−6609.
(100) Dohm, J. A.; Lee, S. J.; Hardwick, J. M.; Hill, R. B.; Gittis, A. G. Cytosolic Domain of the Human Mitochondrial Fission Protein Fis1 Adopts a TPR Fold. *Proteins: Struct., Funct., Genet.* **2004**, *54*, 153−156.

DOI: 10.1021/acscentsci.7b00338
ACS Cent. Sci. 2017, 3, 1156−1167